

## Investigation of Crystallization Kinetic Parameters of $\text{Li}_2\text{O-Al}_2\text{O}_3\text{-SiO}_2$ Glass Ceramic in presence of Various Nuclei

<sup>1</sup>Narmin Montakhab, <sup>2</sup>Parisa Sowti Khiabani, <sup>3</sup>Mohammad Rezvani

<sup>1</sup>Department of Materials Engineering, Faculty of Mechanical Engineering, University of Tabriz, Tabriz, Iran

**ABSTRACT:** The effect of  $\text{Y}_2\text{O}_3$ ,  $\text{CeO}_2$ ,  $\text{P}_2\text{O}_5$ ,  $\text{ZrO}_2$  and  $\text{TiO}_2$  in single, double, triple and quadruple forms on crystallization mechanism of  $\text{Li}_2\text{O-Al}_2\text{O}_3\text{-SiO}_2$  (LAS) glass-ceramic system is investigated in this article. Nucleation and crystallization temperatures of optimized samples in each form were determined by Ray & Day method. The crystalline phase and microstructures of samples were studied by X-ray diffraction (XRD) analysis and Scanning Electron Microscopy (SEM) images, respectively. Activation energy of crystallization,  $E$ , Avrami and kinetic constants ( $n$ ,  $m$ ) were determined by using Differential Thermal Analysis (DTA) and Marotta and Augis-Bennet methods. According to the obtained kinetic parameters ( $m, n$ ), glasses contained both  $\text{ZrO}_2$  and  $\text{TiO}_2$  nuclei showed bulk crystallization. The samples contained  $\text{ZrO}_2$ ,  $\text{TiO}_2$  and  $\text{CeO}_2$  in the triple nuclei forms, showed two-dimensional bulk crystallization mechanism. Lowest activation energy of crystallization,  $E$  (255.5KJ/mol), and highest Avrami constant,  $n$  (4.38), were obtained from the sample contained 3wt%  $\text{TiO}_2$  and 1wt%  $\text{ZrO}_2$ . Lattice constants of the main phase ( $\beta$ -eucryptite solid solution) in the obtained samples were determined according to their XRD results.

**Keywords:** LAS glass ceramics; Eucryptite; h-quartz; Kinetic parameters; nucleation and crystallization mechanism

### I. INTRODUCTION

Glass-ceramic materials are mainly produced via two controlled stages of nucleation and crystallization. These materials have some advantages, such as minimal or even zero porosity and homogeneous microstructure, over the ceramics that are produced via powder metallurgy [1]. These advantageous properties are achieved by precipitating a large percentage of desired crystal phases (at least 50% vol.) in glass-ceramics[2].

Lithium aluminum silicate (LAS) glass-ceramics are one of the most important glass-ceramic systems which have been extensively investigated and commercialized because of their low (zero or negative) thermal expansion coefficient as well as excellent thermal and chemical durability [3-10].

The most important stable crystalline phases in LAS glass-ceramic systems are Eucryptite, Spodumene, Petalite and meta-stable solid solutions such as  $\beta$ -Eucryptite (h-quartz) and Keatite (tetragonal  $\text{SiO}_2$ ) [1]. Investigations have shown that the most effective nucleating agents in these systems are  $\text{TiO}_2$ ,  $\text{ZrO}_2$ ,  $\text{Fe}_2\text{O}_3$ ,  $\text{Cr}_2\text{O}_3$ ,  $\text{NiO}$ ,  $\text{ZnO}$ ,  $\text{V}_2\text{O}_5$ ,  $\text{P}_2\text{O}_5$  and  $\text{Ta}_2\text{O}_5$ [11].

Sung et al [12] have introduced  $\text{TiO}_2$  as an effective nucleating agent in  $\text{Li}_2\text{O-Al}_2\text{O}_3\text{-SiO}_2$  glass-ceramic systems. According to their results, the crystallization activation energy of a sample containing 3.85 wt%  $\text{TiO}_2$  was 299 (kJ/mol). M. Guedes et al [13]

found that for samples containing a combination of  $\text{TiO}_2$  and  $\text{ZrO}_2$  nucleating agents, the Avrami constant,  $n$ , would change from 1 to 3 by varying the crystallization activation energy from 132 to 195.8 (kJ/mol). However Min and Hu et al [14-15] reported crystallization activation energy was varied from 303 to 425 (kJ/mol) and Avrami constant was 2.8 in a system with the same nuclei. Zheng et al [16] showed the activation energy for crystallization of a sample containing  $\text{TiO}_2$  (2.3 wt %),  $\text{ZrO}_2$  (2 wt %) and  $\text{Y}_2\text{O}_3$ (4.46 wt%) was 512 (kJ/mol).

There are several methods for determining the crystallization mechanism in glass-ceramics such as Marotta [17], Matusita [18], Modified Kissinger [19] and Augis-Bennett [15].

In this research work, the crystallization mechanism and activation energy in  $\text{Li}_2\text{O-Al}_2\text{O}_3\text{-SiO}_2$  glass ceramic systems, containing a mixture of  $\text{TiO}_2$ ,  $\text{ZrO}_2$ ,  $\text{P}_2\text{O}_5$ ,  $\text{CeO}_2$  and  $\text{Y}_2\text{O}_3$  (in a single, double, triple and quadruple nuclei forms) were investigated by using various methods through differential thermal analysis(DTA), Marotta and Augis-Bennett methods.

### II. EXPERIMENTAL PROCEDURE

In this article a glass which is mentioned as S with the composition showed in table 1 was used as the base glass. In all other samples the letters T, Z, Y and C, show presence of  $\text{TiO}_2$ ,  $\text{ZrO}_2$ ,  $\text{Y}_2\text{O}_3$  and  $\text{CeO}_2$  respectively with the indication of their weight percent in front of them. The amount of added nuclei is also shown in table 1.

Sample	Oxides										
	$\text{SiO}_2$	$\text{Al}_2\text{O}_3$	$\text{Li}_2\text{O}$	$\text{Na}_2\text{O}$	$\text{K}_2\text{O}$	$\text{MgO}$	$\text{ZnO}$	$\text{TiO}_2$	$\text{ZrO}_2$	$\text{Y}_2\text{O}_3$	$\text{CeO}_2$
S	66.4	23.04	5.2	0.6	0.6	2.08	2.08	-	-	-	-
$\text{ST}_3$	66.4	23.04	5.2	0.6	0.6	2.08	2.08	3	-	-	-
$\text{ST}_3\text{Z}_1$	66.4	23.04	5.2	0.6	0.6	2.08	2.08	3	1	-	-
$\text{ST}_3\text{Z}_1\text{Y}_1$	66.4	23.04	5.2	0.6	0.6	2.08	2.08	3	1	1	-
$\text{ST}_3\text{Z}_1\text{C}_3$	66.4	23.04	5.2	0.6	0.6	2.08	2.08	3	1	-	3

**Table1.** Chemical composition of glasses (weight percentage)

The raw materials were reagent grade  $\alpha\text{-Al}_2\text{O}_3$  (PB-502 Alumina, Martinswerk Company,  $d_{50} < 45 \mu\text{m}$ ),  $\text{SiO}_2$  (with purity up to 99%,  $d_{50} < 45 \mu\text{m}$ ) and  $\text{Li}_2\text{CO}_3$ ,  $\text{NaCO}_3$ ,  $\text{K}_2\text{CO}_3$ ,  $\text{Mg(OH)}_2$ ,  $\text{ZnO}$ ,  $\text{TiO}_2$ ,  $\text{ZrO}_2$ ,  $\text{P}_2\text{O}_5$ ,  $\text{Y}_2\text{O}_3$  and  $\text{CeO}_2$  were purchased from Merck Company and used without further purification. The mixture of raw materials after mixing thoroughly were transferred to an alumina crucible and melted at 1650°C for 2 hours in an electric furnace. Afterwards the melt was cast in pre-heated stainless steel moulds and cooled naturally to room temperature. The thermal behavior of glass samples was monitored by DTA technique utilizing a simultaneous thermal analyzer (DTG-60 AH Shimadzu). Nucleation temperature ( $T_n$ ),

crystallization peak temperature ( $T_p$ ), crystallization activation energy ( $E$ ), Avrami constant ( $n$ ) and kinetic constant ( $m$ ) were determined from DTA results. The reference material in these experiments was  $\alpha$ - $\text{Al}_2\text{O}_3$  powder and heating rates were 10.5, 12.5, 15 and 17.5°C/min. Dilatometric softening temperatures ( $T_d$ ) and Thermal Expansion Coefficient (TEC) were also measured by a dilatometer (model E-402 Netzsch). The optimum nucleation temperatures of samples were determined by Ray & Day method [20]. An X-ray diffractometer (Siemons-D500) was used in order to identify the produced crystalline phases in heat-treated samples. Cu- $\alpha$  radiation was used with a 20 kV emitter. The samples were polished and etched in 5%HF solution for 30 seconds and then coated with a thin film of gold for evaluation of particle shapes in samples by using a scanning electron microscope (LEO 440i). The lattice parameters of hexagonal  $\beta$ -Eucryptite solid solution were determined by using the following formula [8]:

$$d_{hkl}^2 = \frac{a^2}{\frac{4}{3}(h^2 + hk + k^2) + l^2 \frac{a^2}{c^2}} \quad (1)$$

In which  $d$ ,  $(hkl)$  and  $(a,c)$  refer to distance between lattice planes ( $d$ -spacing), Miller index and lattice parameters.

### III. RESULTS AND DISCUSSION

The base glass sample used in this article (S) is composed of  $\text{SiO}_2$ ,  $\text{Al}_2\text{O}_3$ ,  $\text{Li}_2\text{O}$ ,  $\text{Na}_2\text{O}$ ,  $\text{K}_2\text{O}$ ,  $\text{MgO}$  and  $\text{ZnO}$ . The effect of these compounds on properties of silicate glass has been investigated by several researchers thoroughly. X. Guo, et al [11] has studied the effect of  $\text{Na}_2\text{O}$ ,  $\text{K}_2\text{O}$  and  $\text{MgO}$  on silicate glass. They found that presence of  $\text{Na}_2\text{O}$  and  $\text{K}_2\text{O}$  in the base composition of the glass increases non-bridging oxygen ions and also accelerates the bulk nucleation and subsequent crystallization. However it was found that it decreases the viscosity. Similarly presence of  $\text{MgO}$  at high temperatures showed the same effect on viscosity. H. Bach, et al [21] has found that  $\text{ZnO}$  can improve the workability of silicate glass. In addition, it was found that replacement of  $\text{ZnO}$  with  $\text{Li}_2\text{O}$  decreases the thermal expansion coefficient. However replacement with  $\text{MgO}$  showed the opposite effect. Also he has reported the amount of  $\text{Al}_2\text{O}_3$  must be in the range of 18-25wt% in order to provide the low thermal expansion coefficient, produce a transparent glass and also prevent Mullite phase formation. Furthermore he has found that the high amount of  $\text{SiO}_2$  might increase the viscosity and cause non-homogeneity in this kind of glass ceramic.

In this article, in the first step, in order to investigate the effect of nuclei type and amount, several nuclei were added to the composition of the base glass in various weight percent. According to Ray and Day method [20] the sample with sharpest crystallization peak and highest intensity is mentioned as the optimized one in each group. This sharp and intense peak shows existence of high concentration of an effective nucleating agent and subsequently high value of growth rate. Also according to this method, for the two curves with the same sharpness, the one with lower peak temperature would be considered as the optimized one. The obtained results indicate that the sample containing 3wt %  $\text{TiO}_2$  which is mentioned as  $\text{ST}_3$  was the optimized sample. Fig 1 represents DTA curves of samples containing various

amount of  $\text{TiO}_2$ . Each curve showed only one exothermic peak which is associated with precipitation of  $\beta$ -Eucryptite which is called high quartz solid solution (h-quartz).

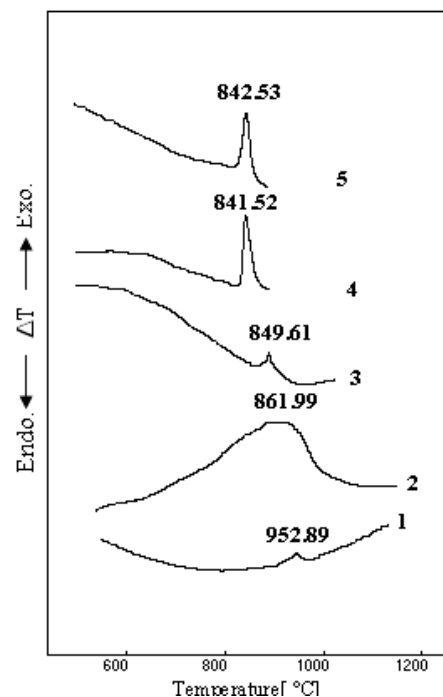


**Fig.1** DTA curves of the glasses S(1),  $\text{ST}_1$ (2),  $\text{ST}_2$ (3),  $\text{ST}_3$ (4) and  $\text{ST}_4$ (5) at the heating rate of 10 (°C/min)

Presence of low concentrations of  $\text{TiO}_2$  as a nucleating agent decreases the crystallization activation energy and thus causes the  $\beta$ -Eucryptite to  $\beta$ -spodumene transformation. At the same time it decreases the viscosity and melting point of the glass [22]. The obtained results showed that the crystallization temperature decreases from 925 to 841°C with increasing  $\text{TiO}_2$  amount from 1 to 3 wt%, whereas increasing up to 4 wt% does not have a significant effect on this temperature. However it decreases the intensity of the crystallization peak. Also presence of  $\text{TiO}_2$  as a nucleating agent causes phase separation. Doherty [23] showed that the phase separation occurred during cooling from the melt and subsequent heating, causes the formation of a large number of Aluminium Titanate crystals ( $\text{Al}_2\text{Ti}_2\text{O}_7$ ) in  $\text{SiO}_2$ -poor regions. These crystals act as sites for heterogeneous nucleation and h-quartz phase formation [21, 24]. So the peaks on DTA curves refer to the formation of h-quartz, which is confirmed by X-ray diffraction results. The same method was used for samples containing various amounts of  $\text{ZrO}_2$ . DTA curves of these samples are represented in Fig 2. Similar to  $\text{TiO}_2$  case, each curve shows an exothermic peak which its intensity reduces gradually with increasing the amount of  $\text{ZrO}_2$ . The presence of  $\text{ZrO}_2$  as a nucleating agent increases the viscosity of the melt as well as the crystallization activation energy, which shifts the peak temperature up to high values and also encourages the formation of  $\beta$ -Spodumene. So the sample containing 1wt %  $\text{ZrO}_2$  which is mentioned as  $\text{SZ}_1$  was chosen as the optimized sample in this group. Results showed that  $\text{TiO}_2$  is more appropriate than  $\text{ZrO}_2$  as a nucleating agent, because of the high power of ionic field of  $\text{Ti}^{4+}$  (1.25) in comparison with  $\text{Zr}^{4+}$  (0.78) and more ion absorption from

nearest neighboring atoms which increases the phase separation. Another problem with  $ZrO_2$  oxides is their weak solubility in silicate melts which limits the amount of  $ZrO_2$  that can be used as a nucleating agent to 3-4 Wt%. Furthermore, in comparison with  $TiO_2$ , the melt contains  $ZrO_2$  as a nucleating agent has a high value of viscosity. So the high viscosity of  $ZrO_2$  in glass melt increases the crystallization activation energy and decreases the crystallization rate and subsequently shifts the peak temperature up to high values [25].

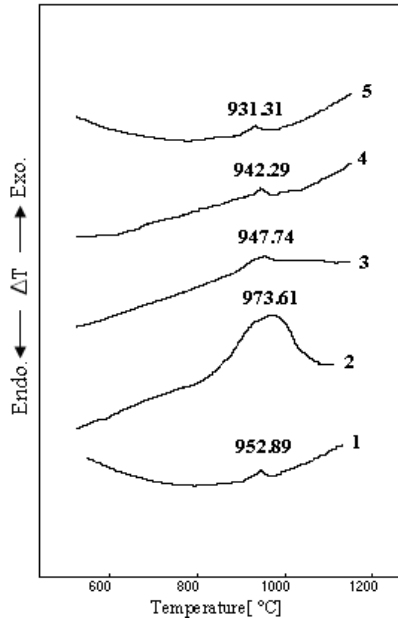


**Fig.2** DTA curves of the glasses S (1),  $SZ_1$  (2),  $SZ_2$ (3), $SZ_3$ (4) and  $SZ_4$ (5)at the heating rate of 10(°C/min)

The same method was used for samples containing  $P_2O_5$ ,  $Y_2O_3$  and  $CeO_2$  as single nucleating agents.

Results showed wide and indeterminate peaks for samples containing various amounts of  $P_2O_5$ . Using this nucleating agent results in direct formation of  $\beta$ -Spodumene without transformation to  $\beta$ -Eucryptite and also decreasing crystallization temperature. For samples containing  $Y_2O_3$  as a nucleating agent, just a sample with 1wt%  $Y_2O_3$  showed the peak with low intensity which vanished with increasing the amount of this agent. Also the results did not show any sharp peak for samples containing  $CeO_2$  as a nucleating agent.

Therefore our investigations showed that  $ST_3$  (the sample contains 3Wt %  $TiO_2$ ) was the best composition among the samples containing single nucleating agent.

In the second step  $ZrO_2$ ,  $P_2O_5$ ,  $Y_2O_3$  and  $CeO_2$  (1-4 wt %) were mixed with  $ST_3$  and used as double (two-component) nucleating agents. According to DTA curves which are shown in Fig 3 and Ray and Day method, sample contained  $TiO_2$  along with 1wt %  $ZrO_2$  as nucleating agents (mentioned as  $ST_3Z_1$ ), showed better crystallization activation energy.

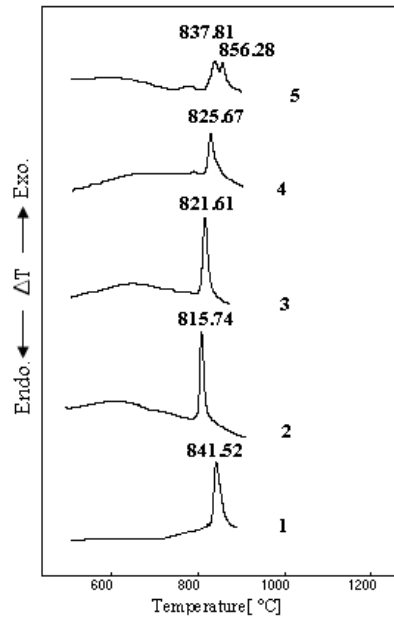


**Fig.3** DTA curves of the glasses  $ST_3$  (1),  $ST_3Z_1$  (2),  $ST_3Z_2$  (3),  $ST_3Z_3$  (4) and  $ST_3Z_4$  (5) at the heating rate of 10(°C/min)

It can be seen that the crystallization temperature decreases from 841°C for  $ST_3$  to 815°C for  $ST_3Z_1$ . However by increasing  $ZrO_2$  amount, the temperature increases slowly up to just below the  $ST_3$  peak temperature and the intensity of the peaks decreases. Two peaks can be seen for  $ST_3Z_4$ . It is assumed that the first one refers to the formation of h-quartz and the second one refers to the transformation of h-quartz to  $\beta$ -Spodumene [26-27]. Hsu et al. [24] found that  $TiO_2$  and  $ZrO_2$  act as nucleating agents and cause phase separation by precipitating as  $ZrTiO_4$  phase in  $SiO_2$ -poor regions. As contrast, Maier et al. [3] studied a lithium aluminosilicate glass containing  $TiO_2+ZrO_2$ . They also observed the formation of  $ZrTiO_4$  crystallites which acted as precursor nuclei for subsequent crystallization. Fig 4 represents the phase separation in  $ST_3Z_1$  glass ceramic.

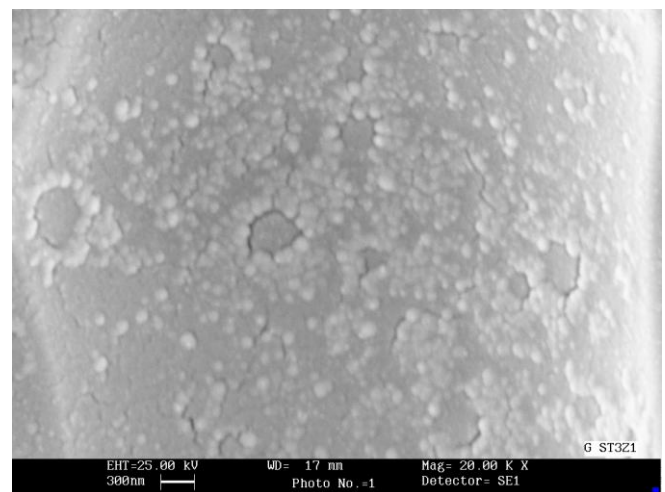


**Fig.4** SEM micrograph of  $ST_3Z_1$  glass that represents the separated regions in glass matrix

Results showed that the simultaneous use of  $TiO_2$  and  $P_2O_5$  as nucleating agents could not improve the nucleation rate and no sharp peak in DTA curves was observed. Also the

crystallization temperature increased and the intensity of the peak decreased by simultaneous use of  $\text{TiO}_2$  and  $\text{Y}_2\text{O}_3$  as double nucleating agents.

Hu et al [28] found that  $\text{CeO}_2$  has a significant role in decreasing viscosity and encouraging the crystallization process as a flux in LAS glass-ceramics. They found that addition of  $\text{CeO}_2$  not only lowers the viscosity of the glass, but also promotes crystallization. However it accelerates the transformations of glass to h-quartz and h-quartz to  $\beta$ -Spodumene. Our results showed that the presence of  $\text{CeO}_2$  decreased the intensity of the crystallization peak so  $\text{TiO}_2$ - $\text{CeO}_2$  couple is not appropriate as a double nucleating agent in LAS glass ceramics.

However our investigations showed that  $\text{ST}_3\text{Z}_1$  (the sample contains 3Wt%  $\text{TiO}_2$  and 1Wt%  $\text{ZrO}_2$ ) was the best composition between samples contain double nucleating agent.

In the third step  $\text{P}_2\text{O}_5$ ,  $\text{Y}_2\text{O}_3$  and  $\text{CeO}_2$  (1-4 wt %) were added to  $\text{ST}_3\text{Z}_1$  in order to investigate the effect of triple nucleating agents on crystallization mechanism of LAS glass ceramics.  $\text{P}_2\text{O}_5$  didn't show an appropriate result in these series. It seems to be because of its electrical neutralizing effect on  $\text{Al}^{3+}$  in  $\text{AlO}_4$  tetrahedral. According to the results, addition of 1wt%  $\text{Y}_2\text{O}_3$  ( $\text{ST}_3\text{Z}_1\text{Y}_1$ ) and 3wt%  $\text{CeO}_2$  ( $\text{ST}_3\text{Z}_1\text{C}_3$ ) to  $\text{ST}_3\text{Z}_1$  provides better bulk nucleation and crystallization, than other samples in this group.

In the fourth step,  $\text{P}_2\text{O}_5$  and  $\text{CeO}_2$  were added to  $\text{ST}_3\text{Z}_1\text{Y}_1$  and  $\text{ST}_3\text{Z}_1\text{C}_3$  (1-4wt %) in order to investigate the effect of quadruple nucleating agents on crystallization mechanism of these glass ceramics. In both cases crystallization temperature increased (above  $900^\circ\text{C}$ ). Also the sharpness of exo-peaks decreased gradually and eventually the peaks vanished. Therefore the results showed the samples contained quadruple nucleating agents were not appropriate.

$\text{ST}_3\text{Z}_1$ ,  $\text{ST}_3\text{Z}_1\text{Y}_1$  and  $\text{ST}_3\text{Z}_1\text{C}_3$  were chosen as optimized samples. They were kept for 3 hours at several temperatures above their glass transition temperature ( $T_g$ ) i.e.  $600$ - $735^\circ\text{C}$  for  $\text{ST}_3\text{Z}_1$ ,  $684$ - $754^\circ\text{C}$  for  $\text{ST}_3\text{Z}_1\text{Y}_1$  and  $690$ - $740^\circ\text{C}$  for  $\text{ST}_3\text{Z}_1\text{C}_3$ . Then the nucleation temperature ( $T_n$ ) and crystallization temperature ( $T_p$ ) was determined by Ray and Day method according to DTA results of each sample which are shown in figures 5 to 7.

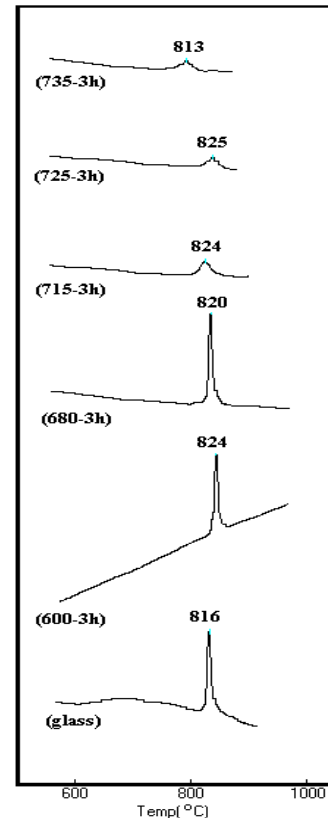


**Fig.5** DTA plots of  $\text{ST}_3\text{Z}_1$  glass heat treated at different temperatures with soaking time for 3 hours (in order to determine the nucleation temperature)

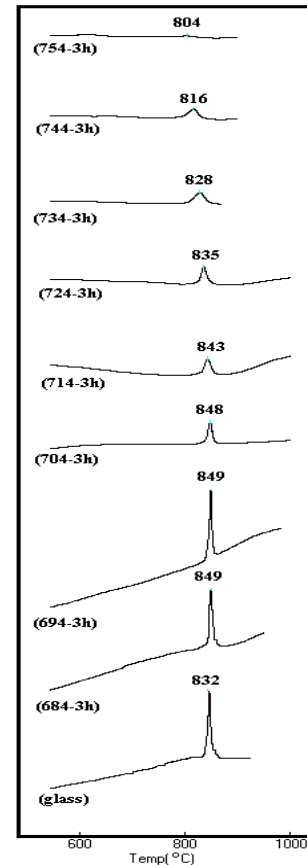


**Fig.6** DTA plots of the  $\text{ST}_3\text{Z}_1\text{Y}_1$  glass heat treated at different temperatures with soaking time for 3 hours (in order to determine the nucleation temperature)

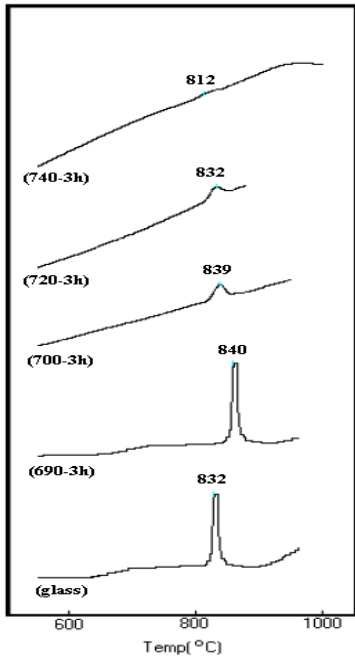


**Fig.7** DTA plots of the  $ST_3Z_1C_3$  glass heat treated at different temperatures with soaking time for 3 hours (in order to determine the nucleation temperature)

According to the results the optimum nucleation temperatures are 680, 694 and 690°C and the optimum crystallization temperatures at these nucleation temperatures are 820, 849 and 840°C for  $ST_3Z_1$ ,  $ST_3Z_1Y_1$ ,  $ST_3Z_1C_3$ , respectively.

Fig 8 represents the XRD patterns of the three optimized samples after 3 hours of heat treatment at their crystallization temperature.

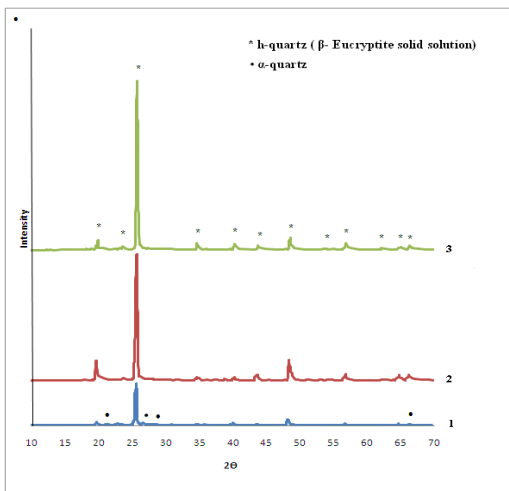


**Fig.8** X-ray diffraction pattern for  $ST_3Z_1C_3$  (1),  $ST_3Z_1Y_1$ (2) and  $ST_3Z_1$  (3) at their DTA peak crystallization temperature for 3 h

As it can be seen, main crystalline phase in all samples is h-quartz ( $\beta$ - Eucryptite). However free quartz ( $\alpha$ -quartz) was detected beside the main phase for  $ST_3Z_1C_3$ . It has been known that formation of free quartz leads to higher Thermal Expansion Coefficients (TEC) and lower

thermal shock resistances in this kind of glass ceramics [29].

As it is presented in XRD results, the intensities of h-quartz peaks decrease by adding  $Y_2O_3$  and  $CeO_2$  to  $ST_3Z_1$ .

The lattice parameters of h-quartz ( $\beta$ -eucryptite solid solution) have been calculated from the measured d-value of crystal plane. The crystal planes of (101), (112) and (100) have been used for determination of lattice parameters which are shown in Table 2. These results are comparable with lattice constants of h-quartz-type and Keatite-type aluminosilicates ( $Zn_{0.5}AlSi_2O_6$  and  $LiAlSi_2O_6$  composition) [21]. Therefore, it can be deduced that the optimized samples should have a low thermal expansion coefficient of about  $1.7 \times 10^{-6} / ^\circ C$  because of their approximately equal lattice constants to the above-mentioned compositions. Thermal expansion coefficients of the optimized samples were measured by dilatometer test between room temperature ( $T_R$ ) and dilatometric softening temperature ( $T_d$ ).

**Table2.** Unit-cell dimension for optimum samples and various h-quartz type alumina-silicates

Composition	Lattice Constants, °A	
	a	c
$ST_3Z_1$	5.200	5.434
$ST_3Z_1Y_1$	5.221	5.661
$ST_3Z_1C_3$	5.208	5.850
$LiAlSi_2O_6$	5.212	5.457
$Zn_{0.5}AlSi_2O_6$	5.220	5.460

Coefficient of linear thermal expansion – the linear thermal expansion per temperature change- is represented in the following equation (2):

$$\alpha = \frac{\Delta L / L_1}{\Delta T} = \frac{L_2 - L_1}{L_1(T_2 - T_1)} \quad (2)$$

Where  $L_1$  and  $L_2$  are the lengths of the specimen at the test temperatures of  $T_1$  and  $T_2$  [30]. The dilatometric curves of these samples are shown in Fig 9. Dilatometric softening temperature ( $T_d$ ), glass transition temperature ( $T_g$ ) and thermal expansion coefficient ( $\alpha$ ) for the optimized samples are summarized in table 3.

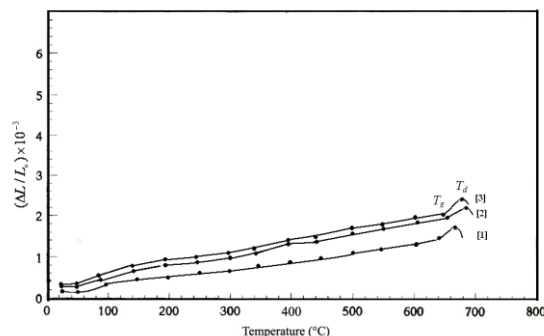


**Fig.9** Dilatometric curves for  $ST_3Z_1$  (1),  $ST_3Z_1Y_1$  (2) and  $ST_3Z_1C_3$  (3)

**Table3.** Dilatometric softening temperature ( $T_d$ ), glass transition temperature ( $T_g$ ) and thermal expansion coefficient ( $\alpha$ ) for the optimized samples

Sample Name	$T_d(^{\circ}\text{C})$	$T_g(^{\circ}\text{C})$	$\alpha (\times 10^{-6}/^{\circ}\text{C})$
ST <sub>3</sub> Z <sub>1</sub>	640	671	1.65
ST <sub>3</sub> Z <sub>1</sub> Y <sub>1</sub>	656	686	1.73
ST <sub>3</sub> Z <sub>1</sub> C <sub>3</sub>	650	680	1.93

Thermal expansion coefficient of ST<sub>3</sub>Z<sub>1</sub> showed the smallest amount among these samples which is about  $2.2 \times 10^{-6} / ^{\circ}\text{C}$  smaller than this amount for LAS glass ceramics.

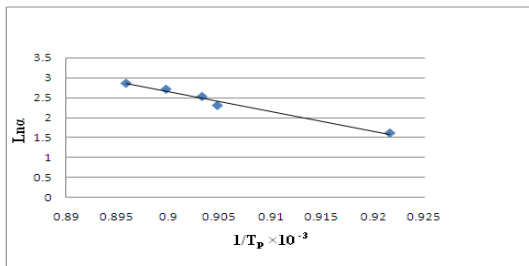
Different methods such as Marotta and Augis-Bennett were used in order to investigate the crystallization mechanism of the optimized samples.

Fig 10 and 11 show the results of variation of  $\text{Ln } \Delta T$  versus  $1/T$  and  $\text{Ln } \alpha$  versus  $1/T_p$  for ST<sub>3</sub>Z<sub>1</sub>Y<sub>1</sub> sample derived from Marotta equations (equation 3 and 4) [17, 31, 28]:

$$\text{Ln}T = \frac{-nE}{RT} + \text{const.} \quad (3)$$

$$\text{Ln}\alpha = \frac{-E}{RT_p} + \text{const.} \quad (4)$$

Where  $\alpha$ ,  $T_p$ ,  $E$ ,  $R$ ,  $n$  and  $\Delta T$  indicate the heating rate, crystallization temperature, crystallization activation energy, gas constant, the value of Avrami constant and temperature deviation from the baseline, respectively. The plots of both patterns are expected to be linear, and value of  $E$  and  $n$  can be measured from the slope of the two lines.



**Fig.10** Variation of  $\text{Ln}\alpha$  vs  $1/T_p$  in ST<sub>3</sub>Z<sub>1</sub>Y<sub>1</sub> for determination of the crystallization activation energy according to Marotta method

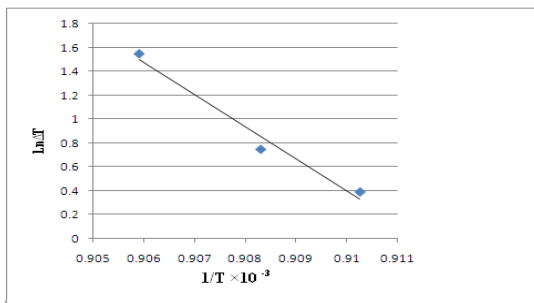


**Fig.11** Variation of  $\text{Ln}\Delta T$  vs  $1/T$  in ST<sub>3</sub>Z<sub>1</sub>Y<sub>1</sub> for determination of the Avrami exponent according to Marotta methods

The crystallization kinetic parameters of the optimized samples can also be calculated by Augis-Bennett equations (equation 5 and 6) which are expressed as below [15]:

$$\text{Ln} \frac{T_p^2}{\alpha} = \frac{E}{RT_p} + \text{const.} \quad (5)$$

$$n = \frac{2.5}{\Delta T} \times \frac{RT_p^2}{E} \quad (6)$$

In this equation,  $\Delta T$  is the width of the exothermic peak at the half maximum intensity. The value of  $n$  close to 1 implies a surface crystallization mechanism,  $n$  close to 2 refers to one-dimensional crystallization,  $n$  close to 3 implies a two-dimensional bulk crystallization process and the value of  $n$  close to 4 implies three-dimensional bulk crystallization [32].

The plot of  $\text{Ln} \frac{T_p^2}{\alpha}$  vs.  $1/T_p$  is shown in Fig 12.

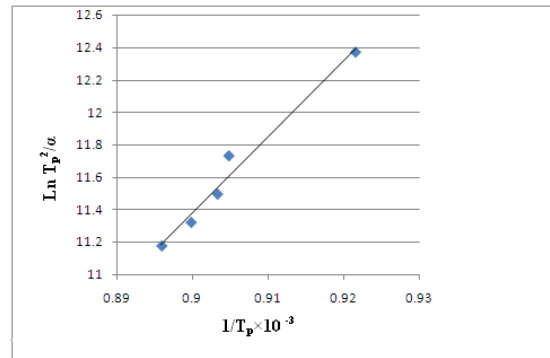


**Fig.12** The plots of  $\text{Ln} \frac{T_p^2}{\alpha}$  vs.  $1/T_p$  for ST<sub>3</sub>Z<sub>1</sub>Y<sub>1</sub> for

determination of the crystallization activation energy according to Augis-Bennett method.

It is used for calculation of the crystallization activation energy and Avrami constant,  $n$ , of the optimized samples which are summarized in Table 4.

**Table4.** Avrami exponent and crystallization activation energy determined by various methods

Sample	Avrami Constant (n)		Activation Energy (E) (kJ/mol)	
	Marotta	Augis-Bennett	Marotta	Augis-Bennett
ST <sub>3</sub> Z <sub>1</sub>	4.23	4.38	269.11	255.2
ST <sub>3</sub> Z <sub>1</sub> Y <sub>1</sub>	3.70	3.81	287.8	273.39
ST <sub>3</sub> Z <sub>1</sub> C <sub>3</sub>	2.96	3.03	365.6	349.67

The  $n$  values determined from the Marotta and Augis-Bennett methods were almost identical. Considering the amount of the Avrami constants were calculated for the optimized samples, it can be deduced that in ST<sub>3</sub>Z<sub>1</sub> and ST<sub>3</sub>Z<sub>1</sub>Y<sub>1</sub> with  $n$  value of about 4, the crystallization

mechanism were three-dimensional which indicates homogeneous crystallization. Therefore the shapes of the crystalline particles in these samples are spherical. Comparison of E values (crystallization activation energy) in  $ST_3Z_1$  and  $ST_3Z_1Y_1$  indicates the same predominate crystallization mechanism. However, it can be seen that  $Y_2O_3$  increases the crystallization activation energy, which would probably leads to a reduction in crystallization rate in  $ST_3Z_1Y_1$  glass ceramics. Comparison of n and E values in  $ST_3Z_1$  and  $ST_3Z_1C_3$  glass ceramics indicates that addition of  $CeO_2$  to the composition increases the crystallization activation energy. Therefore, considering the amounts of the Avrami constants calculated from the Marotta and Augis-Bennett methods in  $ST_3Z_1C_3$  sample, the crystallization mechanism was two-dimensional bulk type and the shapes of the particles were plate like. It should be noted that in spite of the high value of n, the E value was very low, which seems to be the lowest reported for this system [28].

Fig.13 shows the SEM micrograph of  $ST_3Z_1Y_1$  and  $ST_3Z_1C_3$  glass ceramics which have been nucleated at  $T_n$  (optimized nucleation temperature) and crystallized at  $T_p$  (optimized crystallization temperature) for 3 hours.

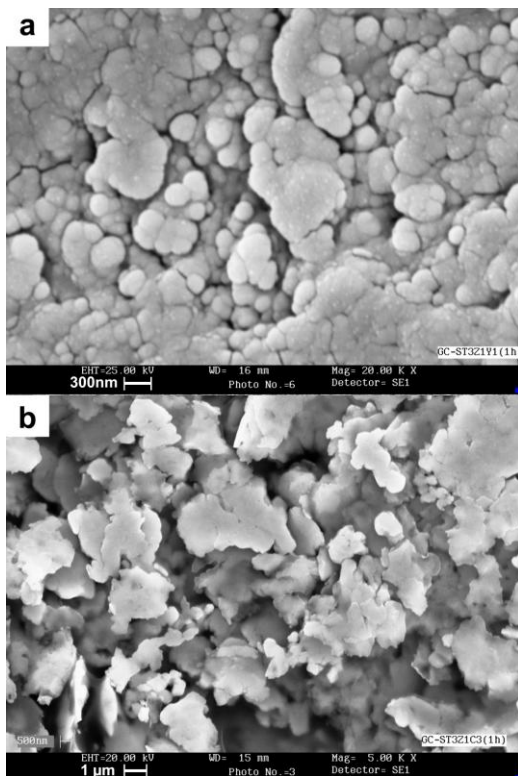


**Fig.13** SEM micrograph of of  $ST_3Z_1Y_1$ (a) and  $ST_3Z_1C_3$  (b) nucleated at  $T_n$  and crystallized at  $T_p$  for 3 h

The presence of plate-like and spherical crystalline particles in morphologies of  $ST_3Z_1C_3$  and  $ST_3Z_1Y_1$  can be seen respectively, which is again an evidence for a two dimensional and three dimensional crystallization mechanisms in these samples respectively. As it can be seen, the precipitated crystalline particles of  $ST_3Z_1Y_1$  are smaller than 300 nm and  $ST_3Z_1C_3$  particles are bigger than 1  $\mu m$ . The fine texture of  $ST_3Z_1Y_1$  which was produced from a suitable nucleating agent would lead to a high bending

strength in this sample. According to the above-mentioned discussion these glass-ceramics can be used as high thermal shock resistance products for commercial applications.

#### IV. CONCLUSIONS

According to DTA results, simultaneous use of  $TiO_2$ ,  $ZrO_2$  and  $CeO_2$  as nucleating agents with various ratios is a proper approach to obtain a high amount of the crystalline phase in bulk crystallization of glass-ceramics in  $Li_2O-Al_2O_3-SiO_2$  systems. The XRD results revealed that the samples are composed of free quartz as the minor phase and h-quartz ( $\beta$ -Eucryptite) as the main phase. The most suitable nucleation temperatures of the optimized samples were 680, 694 and 690°C for  $ST_3Z_1$ ,  $ST_3Z_1Y_1$  and  $ST_3Z_1C_3$ , respectively. The kinetic parameters (m,n) derived from Marotta and Augis-Bennett equations, showed that glass-ceramics containing both  $ZrO_2$  and  $TiO_2$  nuclei, represent bulk crystallization. Also samples containing  $ZrO_2$ ,  $TiO_2$  and  $CeO_2$  in the triple nuclei forms, represent two-dimensional bulk crystallization, which were confirmed by SEM analysis of microstructures of these samples. The minimum crystallization activation energy and maximum Avrami constant were obtained by combination of 3Wt%  $TiO_2$  and 1Wt%  $ZrO_2$  as nucleating agents.

#### V. ACKNOWLEDGMENT

The authors gratefully acknowledge Mr. Nad Ali Arefian for his helpful feedback on the manuscript.

#### VI. REFERENCES

1. McMillan P W. Glass-ceramics. 2nd ed. Non-metallic solids. London ; New York: Academic Press; 1979.
2. Strnad Z E. Glass-ceramic materials : liquid phase separation, nucleation, and crystallization in glasses. Glass science and technology v. 8. Amsterdam ; New York: Elsevier; 1986.
3. Mueller G, Maier V. Mechanism of oxide nucleation in lithium aluminosilicate glass-ceramics. J Am Ceram Soc. 1987;70:C176-C8.
4. Hsu J Y, Speyer R F. Influences of zirconia and silicon nucleating agents on the devitrification of  $Li_2O-Al_2O_3-6SiO_2$  glass. J Am Ceram Soc 1990;73:3583-93.
5. James P F. Glass ceramics: new compositions and uses. Journal of Non-Crystalline Solids. 1995;181(1-2):1-15.
6. Barbieri L, Corradi A B, Leonelli C, Manfredini T, Romagnoli e M, Siligardi C, Mustarelli P, Tomasi C. Nucleation and Crystallization of a Lithium Alumino Silicate Glass. J Am Ceram Soc 1997;80(12):3077-83
7. Beall G H, Beall L R G H , Pinckney L R. Nanophase Glass-Ceramics J Am Ceram Soc 1999;85:5-16
8. Arnault L, Gerland M. Microstructural Study of two LAS-type Glass-Ceramics and Their Parent Glass. J Mat Sci. 2000;35:2331-45.
9. Riello P, Canton P, Comelato N, Polizzi S, Verità M, Fagherazzi G et al. Nucleation and crystallization behavior of glass-ceramic materials in the  $Li_2O-Al_2O_3-SiO_2$  system of interest for their transparency properties. Journal of Non-Crystalline Solids. 2001;288(1-3):127-39.

10. Armakar B, Kundu P, Jana S. Crystallization kinetics and mechanisms of low-expansion lithium-alumino silicate glass-ceramics by dilatometry. *J Am Ceram Soc.* 2002;85(10):2572-4.
11. Guo X, Yang H, Cao M. Nucleation and crystallization behavior of  $\text{Li}_2\text{O}-\text{Al}_2\text{O}_3-\text{SiO}_2$  system glass-ceramic containing little fluorine and no-fluorine. *Journal of Non-Crystalline Solids.* 2005;351(24-26):2133-7.
12. Sung Y-M, Dunn SA, Koutsky JA. The effect of boria and titania addition on the crystallization and sintering behavior of  $\text{Li}_2\text{O}-\text{Al}_2\text{O}_3-4\text{SiO}_2$  glass. *Journal of the European Ceramic Society.* 1994;14(5):455-62.
13. Guedes M, Ferro AC, Ferreira JMF. Nucleation and crystal growth in commercial LAS compositions. *Journal of the European Ceramic Society.* 2001;21(9):1187-94.
14. An-Min H, Kai-Ming L, Fei P, Guo-Liang W, Hua S. Crystallization and microstructure changes in fluorine-containing  $\text{Li}_2\text{O}-\text{Al}_2\text{O}_3-\text{SiO}_2$  glasses. *Thermochimica Acta.* 2004;413(1-2):53-5.
15. Hu AM, Liang KM, Li M, Mao DL. Effect of nucleation temperatures and time on crystallization behavior and properties of  $\text{Li}_2\text{O}-\text{Al}_2\text{O}_3-\text{SiO}_2$  glasses. *Mater Chem Phys.* 2006;98(2-3):430-3. doi:10.1016/j.matchemphys.2005.09.060.
16. Zheng W, Cheng J, Tang L, Quan J, Cao X. Effect of  $\text{Y}_2\text{O}_3$  addition on viscosity and crystallization of the lithium aluminosilicate glasses. *Thermochimica Acta.* 2007;456(1):69-74.
17. Marotta A, Saiello S, Branda F, Buri A. Activation energy for the crystallization of glass from DDTA curves. *J Mater Sci.* 1982;17:105-8.
18. Matusita K, Sakka S. Study on crystallization kinetics in glass by differential thermal analysis. *Thermochimica Acta.* 1979;33(0):351-4.
19. Matusita K, Sakka S. Kinetic study of crystallization of glass by differential thermal analysis—criterion on application of Kissinger plot. *Journal of Non-Crystalline Solids.* 38-39, Part 2(0):741-6.
20. Ray C S, Fang X, Day D E. New Method for Determining the Nucleation and Crystal-Growth Rates in Glasses. *J Am Ceram, Soc.* 2000;83(4):865-72.
21. Bach H. Low thermal expansion glass ceramics. Schott series on glass and glass ceramics. Berlin ; New York: Springer; 1995.
22. Al-Harbi O A, Esmat M A, Hamzawy, Mujtaba Khan M. Effect of Different Concentrations of Titanium Oxide ( $\text{TiO}_2$ ) on the Crystallization Behavior of  $\text{Li}_2\text{O}-\text{Al}_2\text{O}_3-\text{SiO}_2$  Glasses Prepared from Local Raw Materials. *Journal of Applied Sciences.* 2009;9(16):2981-6.
23. Doherty P E, Lee D W, Davis R S. Davis. Direct Observation of the Crystallization of  $\text{Li}_2\text{O}-\text{Al}_2\text{O}_3-\text{SiO}_2$  Glasses Containing  $\text{TiO}_2$ . *J Am Ceram Soc.* 1967;52(2):77-81.
24. Hsu A M, Liang K M, Wang G, Zhou F, Peng F. Effect of nucleating agents on the crystallization of  $\text{Li}_2\text{O}-\text{Al}_2\text{O}_3-\text{SiO}_2$  system glass. vol 3. Dordrecht, PAYS-BAS: Springer; 2004.
25. Nocun M, Baugajski W. Effect of Y-PSZ Additive on the Structure, Thermal Behavior and Mechanical Properties of  $\beta$ -Spodumene Ceramics. Aedermannsdorf, SUISSE: Trans Tech; 1997.
26. Barry TI, Clinton D, Lay LA, Mercer RA, Miller RP. The crystallisation of glasses based on the eutectic compositions in the system  $\text{Li}_2\text{O}-\text{Al}_2\text{O}_3-\text{SiO}_2$ . *Journal of Materials Science.* 1970;5(2):117-26.
27. Coon DN, Neilson RM. Effect of MgO Addition on the Glass Transition Temperature of LAS Glasses. *Journal of Materials Science Letters.* 1988;7(1):33-5.
28. Hu AM, Liang KM, Zhou F, Wang GL, Peng F. Phase transformations of  $\text{Li}_2\text{O}-\text{Al}_2\text{O}_3-\text{SiO}_2$  glasses with  $\text{CeO}_2$  addition. *Ceramics International.* 2005;31(1):11-4.
29. García-Moreno O, Fernández A, Torrecillas R. Solid state sintering of very low and negative thermal expansion ceramics by Spark Plasma Sintering. *Ceramics International.* 2011;37(3):1079-83.
30. Serbena FC, Soares VO, Peitl O, Pinto H, Muccillo R, Zanutto ED. Internal Residual Stresses in Sintered and Commercial Low Expansion  $\text{Li}_2\text{O}-\text{Al}_2\text{O}_3-\text{SiO}_2$  Glass-Ceramics. *Journal of the American Ceramic Society.* 2011;94(4):1206-14. doi:10.1111/j.1551-2916.2010.04220.x.
31. Knickerbocker S, Tuzzolo MR, Lawhorne S. Sinterable  $\beta$ -Spodumene Glass-Ceramics. *Journal of the American Ceramic Society.* 1989;72(10):1873-9.
32. Matusita K, Komatsu T, Yokota R. Kinetics of non-isothermal crystallization process and activation energy for crystal growth in amorphous materials. *Journal of Materials Science.* 1984;19(1):291-6.